

# Supplementary Material

## Electronic Born–Oppenheimer Approximation in Nuclear-Electronic Orbital Dynamics

Tao E. Li<sup>a)</sup> and Sharon Hammes-Schiffer<sup>b)</sup>

*Department of Chemistry, Yale University, New Haven, Connecticut 06520,  
USA*

---

<sup>a)</sup>Electronic mail: tao.li@yale.edu

<sup>b)</sup>Electronic mail: sharon.hammes-schiffer@yale.edu

## S1. INITIAL GEOMETRIES FOR HCN AND MALONALDEHYDE

HCN (Units: Angstrom)

N 0.0492158067 0.000 0.000

C 1.2046693425 0.000 0.000

H 2.1221148508 0.000 0.000

Malonaldehyde (Units: Angstrom; Gh: additional proton basis centers)

O 0.0000000000 -1.3008730953 2.0456624985

O 0.0000000000 1.2908329047 2.0456624985

C 0.0000000000 -1.2160310953 0.7592594985

C 0.0000000000 1.2059909047 0.7592594985

C 0.0000000000 -0.0050200953 0.0533444985

H 0.0000000000 -0.0050200953 -1.0248235015

H 0.0000000000 -2.1631460953 0.2189674985

H 0.0000000000 2.1531059047 0.2189674985

H 0.0000000000 -0.3010120550 2.3554201375

Gh 0.0000000000 0.0000000000 2.3554165853

Gh 0.0000000000 0.2553440000 2.3869010000

## S2. ADDITIONAL SIMULATION RESULTS

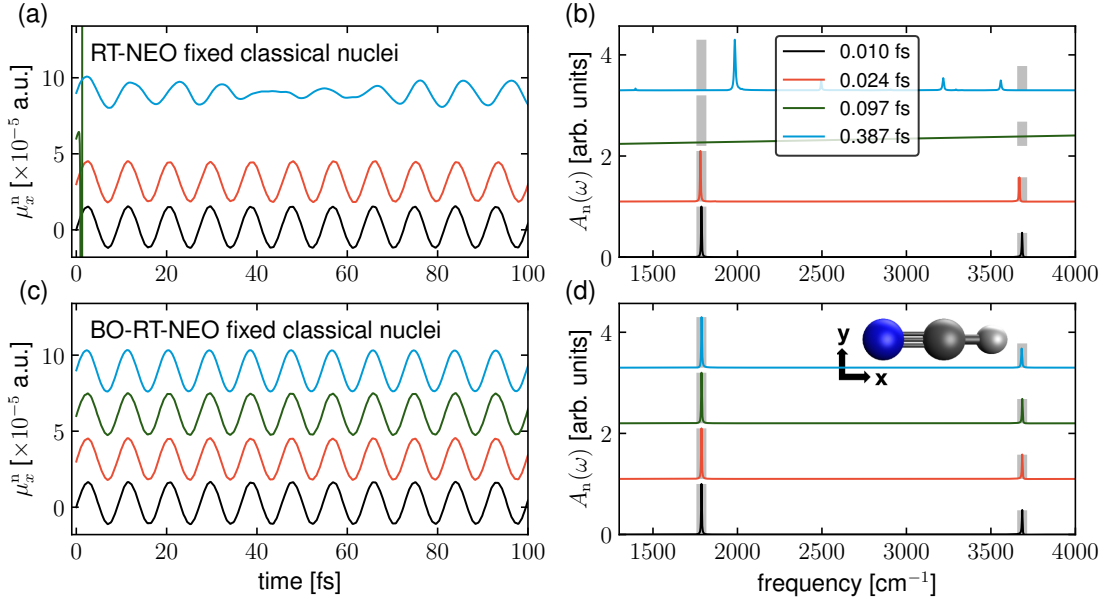


FIG. S1. The same plots as those shown in Fig. 1 except that here the absorption spectrum is plotted:  $A_n = \sum_{i=x,y,z} -\omega \text{Im} [\mathcal{F} [\mu_i^n(t) e^{-\gamma t}]]$ .<sup>S1</sup> The linear-response peak heights (vertical gray solid lines) indicate the absorption intensities. Here, the peak ratios between the real-time signals and the linear-response signals (vertical gray lines) agree exactly.

TABLE S1. Linear-response NEO-TDDFT results for HCN.

| Excite state | Frequency             | Electronic oscillator strength | Protonic oscillator strength |
|--------------|-----------------------|--------------------------------|------------------------------|
| 1            | 1787 cm <sup>-1</sup> | $9.73 \times 10^{-5}$ a.u.     | 0.3559 a.u.                  |
| 2            | 1787 cm <sup>-1</sup> | $9.73 \times 10^{-5}$ a.u.     | 0.3559 a.u.                  |
| 3            | 3685 cm <sup>-1</sup> | $9.56 \times 10^{-5}$ a.u.     | 0.3416 a.u.                  |

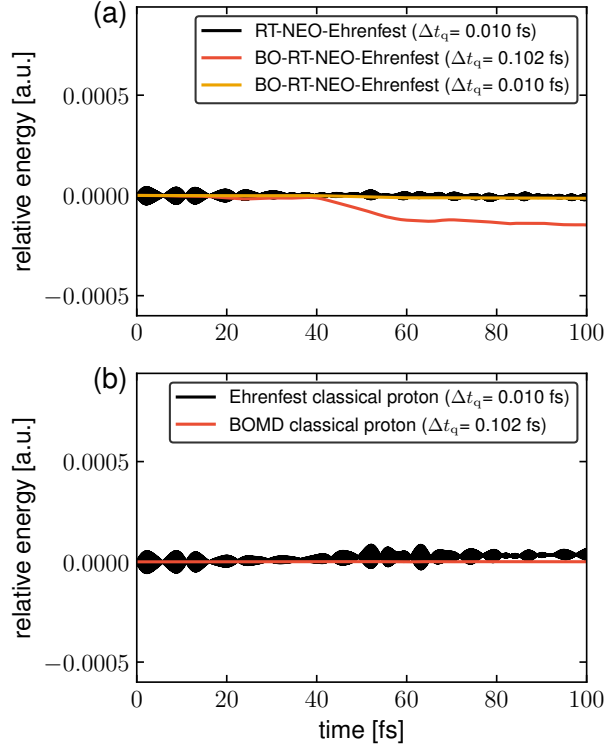


FIG. S2. Energy conservation along the trajectories shown in Fig. 3. For both the NEO and classical simulations, the black lines indicate the trajectories without the BO approximation (with a time step  $\Delta t_q = 0.010$  fs), and the red lines indicate the trajectories with the BO approximation (with a time step  $\Delta t_q = 0.102$  fs). The additional yellow line in part (a) indicates the BO-RT-NEO-Ehrenfest trajectory with the same time step as the RT-NEO-Ehrenfest dynamics (black line), showing that the energy conservation behavior of BO-RT-NEO-Ehrenfest dynamics can be improved by reducing the time step.

### S3. DETAILED ALGORITHMS FOR NEO DYNAMICS

---

**Algorithm S1** Semiclassical BO-RT-NEO dynamics for polaritons with fixed classical nuclei.

---

```

1: Calculate  $\mu_\lambda(\tau = 0) = \text{Tr} [\mathbf{P}^{n'}(\tau = 0)\hat{\mu}_\lambda^{n'}] + 2\text{Tr} [\mathbf{P}^{e'}(\tau = 0)\hat{\mu}_\lambda^{e'}]$ 
2: for  $\tau = \Delta t_q, 2\Delta t_q, \dots$  do
3:   Calculate  $\mu_\lambda(\tau) = \text{Tr} [\mathbf{P}^{n'}(\tau)\hat{\mu}_\lambda^{n'}] + 2\text{Tr} [\mathbf{P}^{e'}(\tau)\hat{\mu}_\lambda^{e'}] - \mu_\lambda(\tau = 0)$ 
4:    $p_{k,\lambda}(\tau + \frac{1}{2}\Delta t_q) = p_{k,\lambda}(\tau - \frac{1}{2}\Delta t_q) - [\omega_{k,\lambda}^2 q_{k,\lambda}(\tau) + \varepsilon_{k,\lambda}\mu_{k,\lambda}(\tau)]\Delta t_q$ 
5:    $q_{k,\lambda}(\tau + \Delta t_q) = q_{k,\lambda}(\tau) + p_{k,\lambda}(\tau + \frac{1}{2}\Delta t_q)\Delta t_q$ 
6:    $p_{k,\lambda}(\tau + \frac{1}{2}\Delta t_q) *= e^{-\gamma_c\Delta t_q}$  //cavity loss
7:    $\mathbf{P}^{e(n)'}(\tau) = [\mathbf{S}^{e(n)}]^{-1/2}\mathbf{P}^{e(n)}(\tau)[\mathbf{S}^{e(n)}]^{-1/2}$ 
8:   Build  $\mathbf{F}_{\text{incav}}^{e(n)'}(\tau)$  using  $\mathbf{P}^{e(n)'}(\tau)$  and  $q_{k,\lambda}(\tau)$ 
9:    $\mathbf{F}_{\text{incav}}^{e(n)}(\tau + \frac{1}{2}\Delta t_q) = 2\mathbf{F}_{\text{incav}}^{e(n)}(\tau) - \mathbf{F}_{\text{incav}}^{e(n)}(\tau - \frac{1}{2}\Delta t_q)$ 
10:  counter = 1
11:  while True do
12:     $\mathbf{P}^n(\tau + \Delta t_q) = e^{-i\Delta t_q\mathbf{F}_{\text{incav}}^n(\tau + \frac{1}{2}\Delta t_q)}\mathbf{P}^n(\tau)e^{i\Delta t_q\mathbf{F}_{\text{incav}}^n(\tau + \frac{1}{2}\Delta t_q)}$ 
13:    if scf_e AND counter == 1 then
14:      Converge  $\mathbf{P}^{e'}(\tau + \Delta t_q)$  to ground state given  $\mathbf{P}^{n'}(\tau + \Delta t_q)$ 
15:    else
16:       $\mathbf{P}^e(\tau + \Delta t_q) = e^{-i\Delta t_q\mathbf{F}_{\text{incav}}^e(\tau + \frac{1}{2}\Delta t_q)}\mathbf{P}^e(\tau)e^{i\Delta t_q\mathbf{F}_{\text{incav}}^e(\tau + \frac{1}{2}\Delta t_q)}$ 
17:    end if
18:    Build  $\mathbf{F}_{\text{incav}}^{e(n)'}(\tau + \Delta t_q)$  using  $\mathbf{P}^{e(n)'}(\tau + \Delta t_q)$  and  $q_{k,\lambda}(\tau + \Delta t_q)$ 
19:     $\mathbf{F}_{\text{incav}}^{e(n)}(\tau + \frac{1}{2}\Delta t_q) = \frac{1}{2}\mathbf{F}_{\text{incav}}^{e(n)}(\tau) + \frac{1}{2}\mathbf{F}_{\text{incav}}^{e(n)}(\tau + \Delta t_q)$ 
20:    if counter > 1 then
21:      if  $|\mathbf{P}^{e(n)}(\tau + \Delta t_q) - \mathbf{P}_{\text{test}}^{e(n)}| < \text{thres}$  then
22:        Exit the while loop
23:      end if
24:    end if
25:     $\mathbf{P}_{\text{test}}^{e(n)} = \mathbf{P}^{e(n)}(\tau + \Delta t_q)$ 
26:    counter += 1
27:  end while
28: end for

```

---

---

**Algorithm S2** BO-RT-NEO-Ehrenfest dynamics.

---

```
1:  $\Delta t_{N_q} = \Delta t_N/n$ ,  $\Delta t_q = \Delta t_{N_q}/m$ 
2: for  $t = 0, \Delta t_N, 2\Delta t_N, \dots$  do
3:   if scf_e then
4:     Converge  $\mathbf{P}^{e'}(t)$  to ground state given  $\mathbf{P}^{n'}(t)$ 
5:   end if
6:   Compute forces  $\mathbf{F}(t)$  using  $\mathbf{P}^{e'}(t)$  and  $\mathbf{P}^{n'}(t)$ 
7:    $\mathbf{P}(t + \frac{1}{2}\Delta t_N) = \mathbf{P}(t - \frac{1}{2}\Delta t_N) + \mathbf{F}(t)\Delta t_N$ 
8:    $\mathbf{R}(t + \Delta t_N) = \mathbf{R}(t) + \mathbf{P}(t + \frac{1}{2}\Delta t_N)\Delta t_N/M$ 
9:   for  $j = 1, 2, \dots, n$  do
10:     $t' = t + (j-1)\Delta t_{N_q}$ 
11:     $\mathbf{R}(t' + \frac{1}{2}\Delta t_{N_q}) = \mathbf{R}(t) + ((j-1)\Delta t_{N_q} + \frac{1}{2}\Delta t_{N_q})\mathbf{P}(t + \frac{1}{2}\Delta t_N)/M$ 
12:    Update basis center to  $\mathbf{R}(t' + \frac{1}{2}\Delta t_{N_q})$  and recompute  $\mathbf{S}^{e(n)}$ 
13:    for  $i = 1, 2, \dots, m$  do
14:       $\tau = t + (i-1)\Delta t_q$ 
15:       $\mathbf{P}^{e(n)'}(\tau) = [\mathbf{S}^{e(n)}]^{-1/2}\mathbf{P}^{e(n)}(\tau)[\mathbf{S}^{e(n)}]^{-1/2}$ 
16:      Build  $\mathbf{F}^{e(n)'}(\tau)$  using  $\mathbf{P}^{e(n)'}(\tau)$  and  $\mathbf{R}(t' + \frac{1}{2}\Delta t_{N_q})$ 
17:       $\mathbf{F}^{e(n)}(\tau + \frac{1}{2}\Delta t_q) = 2\mathbf{F}^{e(n)}(\tau) - \mathbf{F}^{e(n)}(\tau - \frac{1}{2}\Delta t_q)$ 
18:      counter = 1
19:      while True do
20:         $\mathbf{P}^n(\tau + \Delta t_q) = e^{-i\Delta t_q[\mathbf{F}^n(\tau + \frac{1}{2}\Delta t_q)]}\mathbf{P}^n(\tau)e^{i\Delta t_q[\mathbf{F}^n(\tau + \frac{1}{2}\Delta t_q)]}$ 
21:        if scf_e AND counter == 1 then
22:          Converge  $\mathbf{P}^{e'}(\tau + \Delta t_q)$  to ground state given  $\mathbf{P}^{n'}(\tau + \Delta t_q)$ 
23:        else
24:           $\mathbf{P}^e(\tau + \Delta t_q) = e^{-i\Delta t_q\mathbf{F}^e(\tau + \frac{1}{2}\Delta t_q)}\mathbf{P}^e(\tau)e^{i\Delta t_q\mathbf{F}^e(\tau + \frac{1}{2}\Delta t_q)}$ 
25:        end if
26:        Build  $\mathbf{F}^{e(n)'}(\tau + \Delta t_q)$  using  $\mathbf{P}^{e(n)'}(\tau + \Delta t_q)$  and  $\mathbf{R}(t' + \frac{1}{2}\Delta t_{N_q})$ 
27:         $\mathbf{F}^{e(n)}(\tau + \frac{1}{2}\Delta t_q) = \frac{1}{2}\mathbf{F}^{e(n)}(\tau) + \frac{1}{2}\mathbf{F}^{e(n)}(\tau + \Delta t_q)$ 
28:        if counter > 1 then
29:          if  $|\mathbf{P}^{e(n)}(\tau + \Delta t_q) - \mathbf{P}_{\text{test}}^{e(n)}| < \text{thres}$  then
30:            Exit the while loop
31:          end if
32:        end if
33:         $\mathbf{P}_{\text{test}}^{e(n)} = \mathbf{P}^{e(n)}(\tau + \Delta t_q)$ 
34:        counter += 1
35:      end while
36:    end for
37:  end for
38: end for
```

---

In the above two algorithms, when the electronic BO approximation is invoked, the parameter `scf_e` is set to `true`, and otherwise this parameter is set to `false`.

The parameter `thres` in the above two algorithms controls the maximal error in the density matrices during each time step. In our simulation, we have set a very loose threshold

$10^{-4}$  a.u.

In RT-NEO-Ehrenfest dynamics, the parameters  $m$  and  $n$  are used to reduce the number of energy gradient evaluations,<sup>S2</sup> which is the most time-consuming step. For our calculations in the manuscript, we have set  $m = 1$  and  $n = 10$ .

### A. Strategies for reducing the computational cost of BO-RT-NEO dynamics

For both algorithms above, one time consuming step is the building of the complex-valued electronic Fock matrix. Under the electronic Born–Oppenheimer (BO) approximation, building the complex-valued electronic Fock matrices in Lines 8 and 18 of Algorithm S1 and in Lines 16 and 26 of Algorithm S2 can be avoided. Instead, only the real-valued electronic Fock matrix needs to be built during the electronic SCF procedure. Although the electronic SCF procedure is time consuming, this strategy allows each BO-RT-NEO-TDDFT time step to be only twice the computational cost of a RT-NEO-TDDFT time step without the BO approximation.

For RT-NEO-Ehrenfest dynamics, the most time consuming step is the gradient evaluation. Under the electronic BO approximation, because the electronic density is always real-valued, it is unnecessary to calculate the gradient components involving the imaginary part of the electronic density. In contrast, for NEO-Ehrenfest dynamics without the electronic BO approximation, the imaginary part of the electronic density should be taken into account for the gradient evaluation. Hence, the computational cost of the gradient evaluation can also be reduced significantly under the electronic BO approximation.

## REFERENCES

- [S1]L. Zhao, Z. Tao, F. Pavošević, A. Wildman, S. Hammes-Schiffer, and X. Li, “Real-Time Time-Dependent Nuclear-Electronic Orbital Approach: Dynamics beyond the Born–Oppenheimer Approximation,” *J. Phys. Chem. Lett.* **11**, 4052–4058 (2020).
- [S2]L. Zhao, A. Wildman, Z. Tao, P. Schneider, S. Hammes-Schiffer, and X. Li, “Nuclear–electronic orbital Ehrenfest dynamics,” *J. Chem. Phys.* **153**, 224111 (2020).